

04.2

Using Thomson scattering diagnostics to control plasma density at Globus-M2 tokamak

© N.S. Zhiltsov¹, G.S. Kurskiev¹, V.A. Solovey², V.K. Gusev¹, A.A. Kavin³, E.O. Kiselev¹,
V.B. Minaev¹, E.E. Mukhin¹, Yu.V. Petrov¹, N.V. Sakharov¹, V.V. Solokha¹, A.N. Novokhatsky¹,
E.E. Tkachenko¹, S.Yu. Tolstyakov¹, E.A. Tukhmeneva¹

¹ Ioffe Institute, St. Petersburg, Russia

² St. Petersburg Nuclear Physics Institute, National Research Center Kurchatov Institute, Gatchina, Russia

³ JSC „NIIIEFA“, St. Petersburg, Russia

E-mail: nisovru@gmail.com

Received May 11, 2023

Revised June 7, 2023

Accepted June 7, 2023

This work describes the real-time application of the Thomson scattering diagnostics. The upgraded data acquisition system of the Globus-M2 spherical tokamak provides real-time data processing with the delay < 2.4 ms for 128 scattering signals from 11 spatial points. The achieved processing performance meets the requirements for Thomson scattering diagnostics of modern thermonuclear facilities and ITER in particular. The paper demonstrates the possibility of plasma electron density control, using Thomson scattering data in the feedback loop.

Keywords: tokamak, Thomson scattering, real-time.

DOI: 10.61011/TPL.2023.08.56688.19625

Plasma diagnostics by Thomson scattering (TS) of laser radiation is a well-established method [1–3] for reliable measurement of the spatial distribution dynamics of electron temperature $T_e(R, t)$ and density $n_e(R, t)$ in tokamak and stellarator plasma. TS data improves localization accuracy for plasma boundary and magnetic axis, reconstructed by equilibrium codes EFIT [4], PET [5], etc. This data also allows one to determine electron stored energy W_e and the ratio of the electron pressure to the magnetic field pressure (β_e). This information must be obtained in real time (RT) to prevent accidents involving plasma current disruption [6]. Real-time TS diagnostics is also needed to implement advanced methods for control over the profiles of plasma density, current, and electron and ion temperatures for optimizing the thermonuclear synthesis yield in tokamak reactors [7,8]. At the ITER tokamak, TS diagnostics is designated to provide feedback for control over hybrid operation modes [6]. The implementation of control over profiles of various plasma parameters is also one of the key goals of the Russian Tokamak with Reactor Technologies (TRT) project [9,10]. TS diagnostics is a promising way toward this goal [11].

A new TS diagnostics complex [12] satisfying the key requirements for ITER TS diagnostics has been put into operation in 2020 at the Globus-M2 tokamak. This complex provides an opportunity to perform measurements in a stationary mode with a frequency of 330 Hz. A total of 11 five-channel polychromators based on interference light filters are used to analyze the spectrum of scattered radiation. Avalanche photodiodes fitted with wide-band (> 250 MHz) transimpedance amplifiers are used as detectors [13]. Eight 16-channel 12-bit CAEN V1743 digitizer VME modules

operating at a sampling frequency of 3.2 GS/s are used to measure the time dependence of laser scattering intensity. All eight digitizers are connected pairwise to a single four-channel CAEN A3818C PCI-e controller in a data acquisition computer. Each preamplifier of an avalanche photodiode has two high-frequency outputs with different gain levels that are meant to expand the dynamic range of measured signals. A total of 110 oscilloscope records of TS signals and eight oscilloscope records of the temporal shape of a probing laser pulse (one per each V1743 module) are made per a single laser pulse (time point). The computer runs on an AMD Ryzen 5 3600X six-core processor and has a general-purpose operating system (OS) installed (specifically, Windows 10). The program for data acquisition and processing was written in C++ and is executed with the highest priority in the OS task manager. One thread is allocated per each of the four lines of communication with digitizers to transfer data from the buffer of digitizers into the computer RAM. The fifth computing thread is allocated for processing and determination of the number of detected photoelectrons in each of the 128 oscilloscope records ($11 \cdot 5 \cdot 2$ TS signals + eight synchronization signals + ten idle channels). A control feedback signal, which is transmitted over an Ethernet network in the form of a UDP packet, is generated after processing of all channels. The packet passes through two switches, reaches Raspberry Pi 4B single-board computer and gets converted into a command for a 12-bit MCP4725 digital-to-analog converter (DAC) connected to an I2C serial communication bus. The DAC outputs a signal to the tokamak data acquisition and control system. The mean electron density was chosen as a controlled parameter in order to demonstrate the application

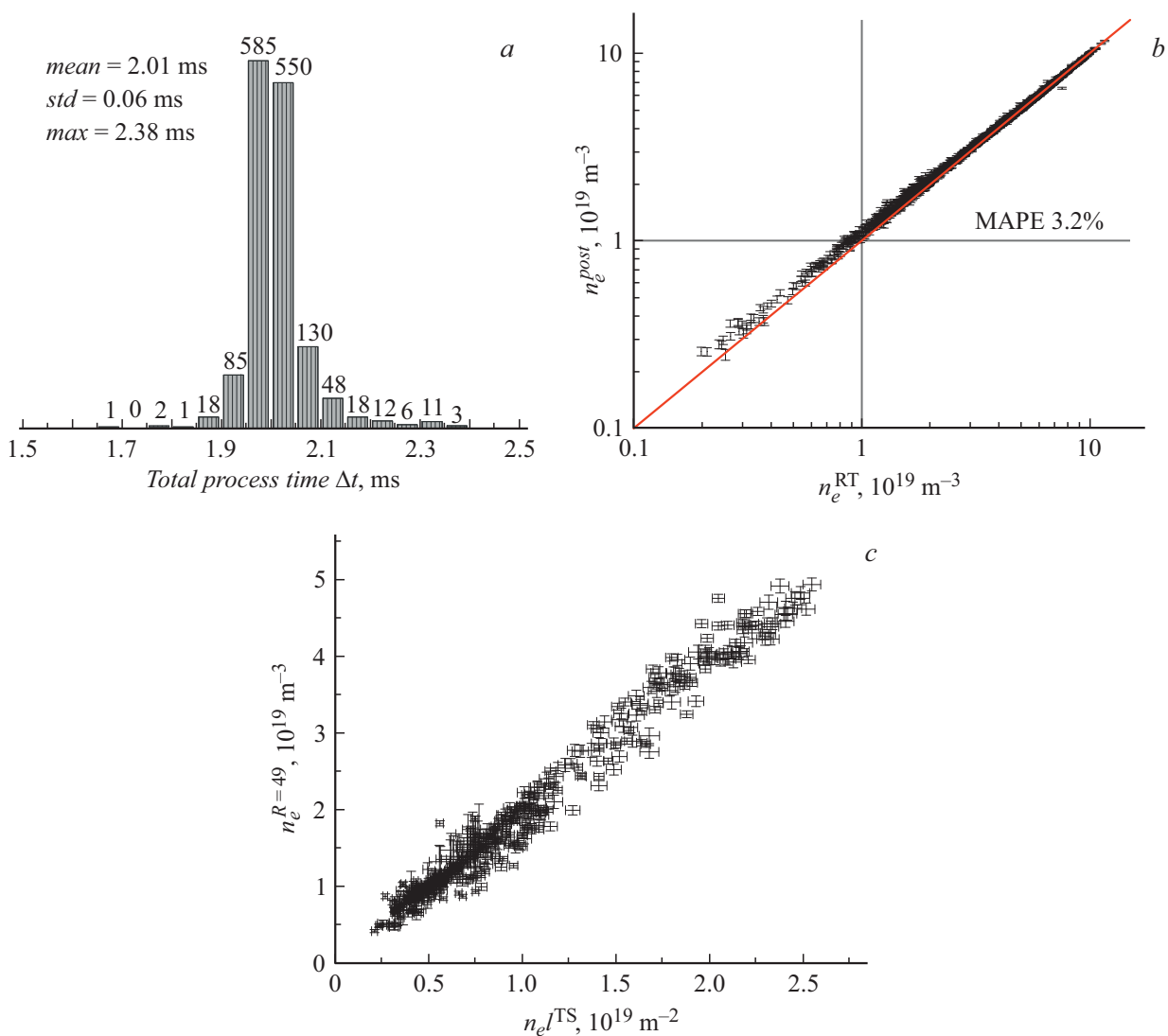


Figure 1. *a* — Histogram of the TS signal processing time elapsed from the moment of plasma probing to the update of control DAC registers (numbers correspond to the number of events falling within a given time interval); *b* — local density n_e obtained as a result of post-processing (ordinate axis) and n_e obtained as a result of RT processing with a simplified code (abscissa axis); *c* — local density at a point with major radius $R = 49$ cm as a function of linear density.

potential of TS diagnostics in the tokamak control system; a MaxTec MV-112 piezoelectric valve, which regulated the hydrogen flow into the chamber, served as an actuator.

A simplified algorithm for TS data processing was developed to calculate the n_e profile in real time. Figure 1, *a* presents the histogram of the calculation cycle operation time in a series of tokamak discharges. The processing time includes the stages of data digitizing, transfer into the computer memory, n_e profile calculation, and transmission of the control signal to the DAC. The mean time was 2.01 ms, while the maximum time did not exceed 2.38 ms; the interval between laser pulses was 3.03 ms. The time spent on data transfer from the digitizer to the computer and from the computer to the DAC was 1.2 and 0.5 ms, respectively; taken together, these operations took 85% of the cycle time. Figure 1, *b* presents a comparison between the results of

calculation of local n_e values obtained using the standard experimental data processing algorithm (post-processing) and the simplified TS data processing algorithm. It is evident that the results produced by these two algorithms agree closely: the mean absolute percentage error (MAPE) is 3.2%. Since RT data on magnetic equilibrium at the Globus-M2 tokamak are currently unavailable, local density $n_e^{R=49}$ measured at a point with major radius $R = 49$ cm (near the middle of the minor radius) was used to set the control parameter. The linear dependence of $n_e^{R=49}$ on $n_e l^{\text{TS}}$ (Fig. 1, *c*) justify the use of local density $n_e^{R=49}$ as an input signal for a proportional mean density regulator in the chosen tokamak operation mode.

The Ohmic mode with a low mean electron density ($< 2 \cdot 10^{19} \text{ m}^{-3}$) and boronization of the first wall was chosen to illustrate the potential for control over the mean

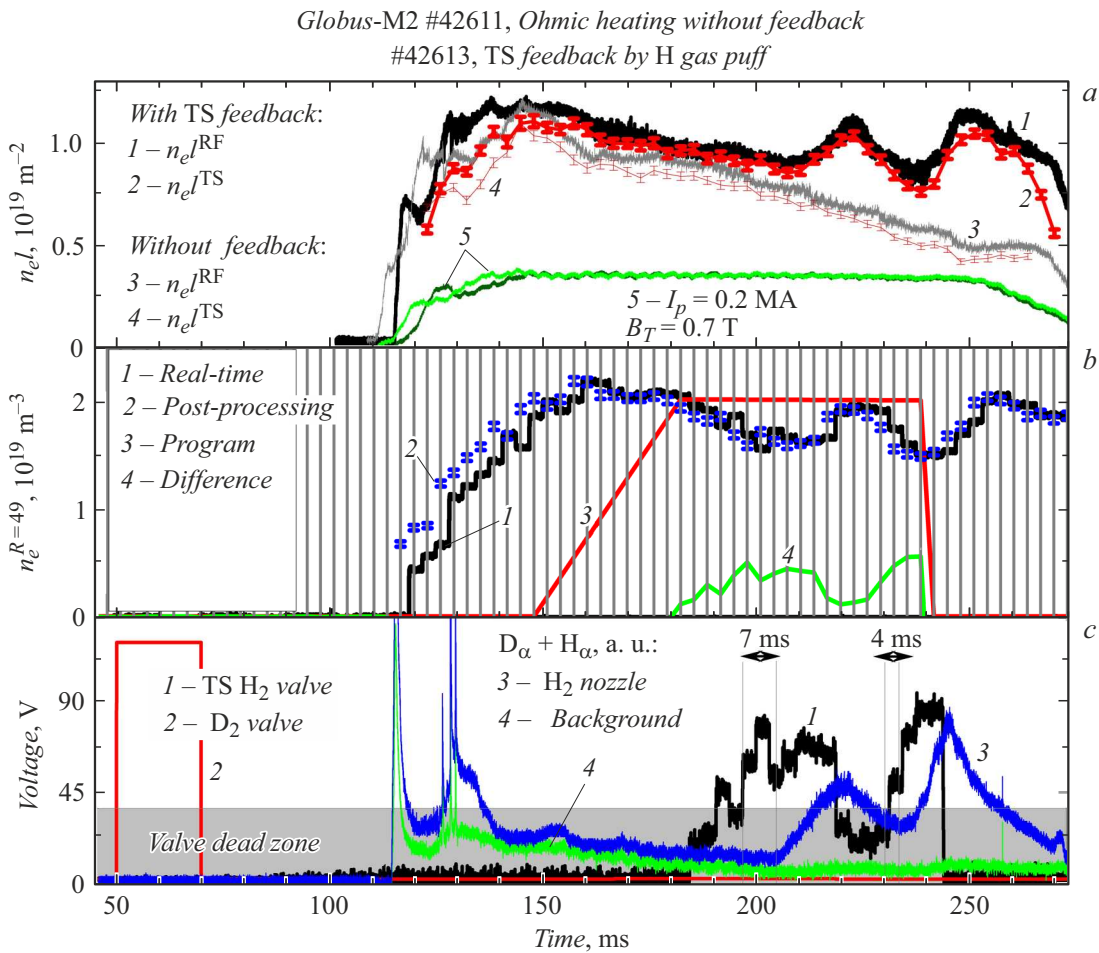


Figure 2. *a* — Integral density determined using a microwave interferometer (1, 3) and the TS method (2, 4). 5 — Plasma current. *b* — Measured local density $n_e^{R=49}$: real-time DAC output (1) and results of post-processing (2). 3 — Pre-set density control program; 4 — difference between the pre-set and measured values. Vertical lines denote the moments of probing. *c* — Piezoelectric valve voltage: 1 — in the feedback circuit; 2 — at the auxiliary valve. The gray area is the valve dead zone. The overall intensity of H_α and D_α emission lines in discharge No. 42613: 3 — for an observation chord directed at the gas puffing nozzle; 4 — for the background signal.

density in the tokamak based on TS diagnostics data. Since a transition to the mode of enhanced confinement, which is accompanied by a sharp change in the particle diffusion coefficient, is not expected to occur in this operation mode of the Globus-M2 tokamak, a simple model of n_e control by a proportional regulator may be used. A short pulse of deuterium puffing via a separate valve was applied in this scenario 50 ms before the discharge to establish breakdown conditions. Figure 2 presents the key plasma parameters for two discharges of the Globus-M2 tokamak: discharge No. 42613 with the density control system switched on and reference discharge No. 42611 without control. All electromagnetic system control programs were identical in these two discharges. The value of $n_e l$ (Fig. 2, *a*) starts decreasing monotonically at 145 ms. Two independent diagnostics were used to measure $n_e l$: the TS method [14] and the microwave interferometer (characteristic chord length $l \approx 0.6$ m). In discharge No. 42613, a control signal (Fig. 2, *c*) was applied to the gas puffing valve when n_e measured using the TS

method dropped to a pre-set level of $n_e^{R=49} = 2 \cdot 10^{19} \text{ m}^{-3}$ (Fig. 2, *b*). This signal was proportional to the difference between the pre-set and measured n_e values. The monotonic $n_e l$ reduction was thus suppressed in the discharge with the n_e control system switched on and responding to a feedback signal from the TS diagnostics system.

The use of a simple proportional controller caused oscillations of the controlled parameter around the pre-set value due to lag of the control system and the controlled plasma. The valve used in our experiments features a dead zone (Fig. 2, *c*) and hysteresis, which were ignored in the process of construction of the controller. The delay between valve opening and gas ionization at the plasma boundary estimated based on the signal of overall intensity of emission lines H_α and D_α (Fig. 2, *c*) was 4–7 ms.

Starting from December 2022, density profiles measured using the TS method are processed in real time at the Globus-M2 tokamak for each plasma discharge. The delay between measurement and the moment when a full profile

is ready does not exceed 2.4 ms; 1.2 ms of this time are spent on data transfer from digitizers, and another 0.5 ms are spent on data transfer to the control DAC. This processing performance is up to world standards [15–17] and satisfies the requirement (2.5 ms) for inclusion of TS diagnostics into the ITER system for control over plasma parameters [6]. The processing time may be reduced to ~ 1 ms by optimizing the data transfer system. A further increase in performance may be achieved by switching to a real-time OS and a high-performance processor. It was demonstrated that the data measured in real time correspond to the results of standard post-processing.

RT processing of TS diagnostics data is implemented in several experiments: KSTAR [18], NSTX-U [16,17], LHD [19,20], MAST [21,22], TCX [23], and DIII-D [24,25]. The use of TS diagnostics data for control over plasma parameters has been mentioned only in [26] as a part of the integral DIII-D tokamak system without any further details. At the same time, the publicly available description of the DIII-D TS diagnostics complex [25,27] does not make any references to the possibility of RT operation, and RT processing is mentioned only as a probable upgrade in an earlier paper [24]. In the present study, the possibility of control over the mean density in a tokamak based on TS diagnostics data in the Ohmic mode with a low mean electron density ($\sim 2 \cdot 10^{19} \text{ m}^{-3}$) was demonstrated. The accuracy of maintaining a certain mean density may be increased qualitatively by optimizing the controller algorithm and the algorithm for control over the working gas puffing valve. The performance of the TS diagnostics system designed for the Globus-M2 tokamak is sufficient for reconstruction of the plasma current profile by equilibrium codes in real time and for systems controlling the spatial distributions of plasma parameters in a tokamak reactor and a neutron source.

Conflict of interest

The authors declare that they have no conflict of interest.

References

- [1] M. Mattioli, *Incoherent light scattering from high temperature plasmas* (Euroatom/CEA, 1974).
- [2] P.E. Stott, G. Gorini, P. Prandoni, E. Sindoni, *Diagnostics for experimental thermonuclear fusion reactors 2* (Springer, N.Y., 1998). DOI: 10.1007/978-1-4615-5353-3
- [3] H.J. van der Meiden, J.W.M. Vernimmen, J. van den Berg, I.G.J. Classen, *J. Fusion Energy*, **39**, 251 (2020). DOI: 10.1007/s10894-020-00262-5
- [4] S.A. Sabbagh, S.M. Kaye, J. Menard, F. Paoletti, M. Bell, R.E. Bell, J.M. Bialek, M. Bitter, E.D. Fredrickson, D.A. Gates, A.H. Glasser, H. Kugel, L.L. Lao, B.P. LeBlanc, R. Maingi, R.J. Maqueda, E. Mazzucato, D. Mueller, M. Ono, S.F. Paul, M. Peng, C.H. Skinner, D. Stutman, G.A. Wurden, W. Zhu and NSTX Research Team, *Nucl. Fusion*, **41**, 1601 (2001). DOI: 10.1088/0029-5515/41/11/309
- [5] S.A. Galkin, A.A. Ivanov, S.Yu. Medvedev, Yu.Yu. Poshek-honov, *Nucl. Fusion*, **37**, 1455 (1997). DOI: 10.1088/0029-5515/37/10/111
- [6] ITER System Requirements Documents for diagnostics (SRD-55) from DOORS (28B39L). Private communication.
- [7] X. Litaudon, E. Barbato, A. Bécoulet, E.J. Doyle, T. Fujita, P. Gohil, F. Imbeaux, O. Sauter, G. Sips, *Plasma Phys. Control. Fusion*, **46**, A19 (2004). DOI: 10.1088/0741-3335/46/5A/002
- [8] M.D. Boyer, D.J. Battaglia, D. Mueller, N. Eidietis, K. Erickson, J. Ferron, D.A. Gates, S. Gerhardt, R. Johnson, E. Kolemen, J. Menard, C.E. Myers, S.A. Sabbagh, F. Scotti, P. Vail, *Nucl. Fusion*, **58**, 036016 (2018). DOI: 10.1088/1741-4326/aaa4d0
- [9] A.V. Krasilnikov, S.V. Konovalov, E.N. Bondarchuk, I.V. Mazul', I.Yu. Rodin, A.B. Mineev, E.G. Kuz'min, A.A. Kavin, D.A. Karpov, V.M. Leonov, R.R. Khayrutdinov, A.S. Kukushkin, D.V. Portnov, A.A. Ivanov, Yu.I. Belchenko, G.G. Denisov, *Plasma Phys. Rep.*, **47**, 1092 (2021). DOI: 10.1134/S1063780X21110192.
- [10] V.M. Leonov, S.V. Konovalov, V.E. Zhogolev, A.A. Kavin, A.V. Krasilnikov, A.Yu. Kuyanov, V.E. Lukash, A.B. Mineev, R.R. Khayrutdinov, *Plasma Phys. Rep.*, **47**, 1107 (2021). DOI: 10.1134/S1063780X21120047.
- [11] G.S. Kurskiev, E.E. Mukhin, A.N. Koval, N.S. Zhil'tsov, V.A. Solovei, S.Yu. Tolstyakov, E.E. Tkachenko, A.G. Rasdobarin, A.M. Dmitriev, A.F. Kornev, A.M. Makarov, A.V. Gorshkov, G.M. Asadulin, A.B. Kukushkin, P.A. Sdvizhenskii, P.V. Chernakov, *Plasma Phys. Rep.*, **48**, 855 (2022). DOI: 10.1134/S1063780X22600487.
- [12] G.S. Kurskiev, N.S. Zhiltsov, A.N. Koval, A.F. Kornev, A.M. Makarov, E.E. Mukhin, Yu.V. Petrov, N.V. Sakharov, V.A. Solovey, E.E. Tkachenko, S.Yu. Tolstyakov, P.V. Chernakov, *Tech. Phys. Lett.*, **48** (15), 78 (2022). DOI: 10.21883/TPL.2022.15.54273.19019.
- [13] G.S. Kurskiev, A.I.P. Chernakov, V.A. Solovey, S.Yu. Tolstyakov, E.E. Mukhin, A.N. Koval, A.N. Bazhenov, S.E. Aleksandrov, N.S. Zhiltsov, V.A. Senichenkov, A.V. Lukoyanova, P.V. Chernakov, V.I. Varfolomeev, V.K. Gusev, E.O. Kiselev, Yu.V. Petrov, N.V. Sakharov, V.B. Minaev, A.N. Novokhatsky, M.I. Patrov, A.V. Gorshkov, G.M. Asadulin, I.S. Bel'bas, *Nucl. Inst. Meth. Phys. Res. A*, **963**, 163734 (2020). DOI: 10.1016/j.nima.2020.163734
- [14] G.S. Kurskiev, N.V. Sakharov, P.B. Shchegolev, N.N. Bakharev, E.O. Kiselev, G.F. Avdeeva, V.K. Gusev, A.D. Ibyaminova, V.B. Minaev, I.V. Miroshnikov, M.I. Patrov, Yu.V. Petrov, A.Yu. Tel'nova, S.Yu. Tolstyakov, V.A. Tokarev, *Vopr. At. Nauki Tekh., Ser. Termoyad. Sint.*, **39** (4), 86 (2016) (in Russian). DOI: 10.21517/0202-3822-2016-39-4-86-94
- [15] M. Kadziela, B. Jablonski, P. Perek, D. Makowski, *J. Fusion Energy*, **39**, 261 (2020). DOI: 10.1007/s10894-020-00264-3
- [16] F.M. Laggner, A. Diallo, B.P. LeBlanc, R. Rozenblat, G. Tchilinguirian, E. Kolemen, NSTX-U Team, *Rev. Sci. Instrum.*, **90**, 043501 (2019). DOI: 10.1063/1.5088248
- [17] R. Rozenblat, E. Kolemen, F.M. Laggner, C. Freeman, G. Tchilinguirian, P. Sicht, G. Zimmer, *Fusion Sci. Technol.*, **75**, 835 (2019). DOI: 10.1080/15361055.2019.1658037
- [18] J.-H. Lee, S.J. Lee, H.J. Kim, S.H. Hahn, I. Yamada, H. Funaba, *Fusion Eng. Des.*, **190**, 113532 (2023). DOI: 10.1016/j.fusengdes.2023.113532

- [19] K.C. Hammond, F.M. Laggner, A. Diallo, S. Doskoczynski, C. Freeman, H. Funaba, D.A. Gates, R. Rozenblat, G. Tchilinguirian, Z. Xing, I. Yamada, R. Yasuhara, G. Zimmer, E. Kolemen, *Rev. Sci. Instrum.*, **92**, 063523 (2021). DOI: 10.1063/5.0041507
- [20] I. Yamada, H. Funaba, J.-H. Lee, Y. Huang, C. Liu, *Plasma Fusion Res.*, **17**, 2402061 (2022). DOI: 10.1585/pfr.17.2402061
- [21] S. Shibaev, G. Naylor, R. Scannell, G.J. McArdle, M.J. Walsh, in *2010 17th IEEE-NPSS Real Time Conf.* (Lisbon, Portugal, 2010), p. 1–6. DOI: 10.1109/RTC.2010.5750394
- [22] S. Shibaev, G. Naylor, R. Scannell, G. McArdle, T. O’Gorman, M.J. Walsh, *Fusion Eng. Des.*, **85**, 683 (2010). DOI: 10.1016/j.fusengdes.2010.03.035
- [23] H. Arnichand, Y. Andrebe, P. Blanchard, S. Antonioni, S. Couturier, J. Decker, B.P. Duval, F. Felici, C. Galperti, P.-F. Isoz, P. Lavanchy, X. Llobet, B. Marlétaz, P. Marmillod, J. Masur, *JINST*, **14**, C09013 (2019). DOI: 10.1088/1748-0221/14/09/C09013
- [24] T.N. Carlstrom, G.L. Campbell, J.C. DeBoo, R. Evanko, J. Evans, C.M. Greenfield, J. Haskovec, C.L. Hsieh, E. McKee, R.T. Snider, R. Stockdale, P.K. Trost, M.P. Thomas, *Rev. Sci. Instrum.*, **63**, 4901 (1992). DOI: 10.1063/1.1143545
- [25] D.M. Ponce-Marquez, B.D. Bray, T.M. Deterly, C. Liu, D. Eldon, *Rev. Sci. Instrum.*, **81**, 10D525 (2010). DOI: 10.1063/1.3495759
- [26] M. Margo, B. Penaflor, H. Shen, J. Ferron, D. Piglowski, P. Nguyen, J. Rauch, M. Clement, A. Battey, C. Rea, *Fusion Eng. Des.*, **150**, 111368 (2020). DOI: 10.1016/j.fusengdes.2019.111368
- [27] R.E. Stockdale, T.N. Carlstrom, C.L. Hsieh, C.C. Makariou, *Rev. Sci. Instrum.*, **66**, 490 (1995). DOI: 10.1063/1.1146326

Translated by D.Safin